04 HAZİRAN 2018

# EE564 – PROJECT 3

## WIND TURBINE DESIGN

FURKAN KARAKAYA
1937051
METU

# Content

# A. INTRODUCTION

In this project, a wind turbine generator is designed analytically and the results are verified in the simulation platform using finite element analysis principles. The analytical design of the generator is started with the design of windings and determination of magnetic and electrical loading. Then, the motor dimensions are specified. For that dimensions and excitations, a simulation model is implemented in RMXPRT and more detailed analysis is conducted in 2D Maxwell Solution.

# B. ANALYTICAL DESIGN

## Motor Dimensions

In Table 1, the design inputs of the wind turbine generator are given. With the given output power and shaft speed, how much torque should be produced by the electrical motor can be calculated.

| | |
|---|---|
| Output Power | 250 kW |
| Turbine Speed | 24.3 rpm |
| Gear Ratio | 31.2 |
| Rated Speed | 758 rpm |
| Line Voltage | 400 Vrms |
| Frequency | 50 Hz |
| Pole Number | 8 |
| Phase Number | 3 |

*Table 1: Design Inputs*

Since the induction motor torque is skew-symmetric around the rated speed, Fig. 1, the induction generator can be considered as in motoring operation with negative rated slip. Therefore, the generator can be designed assuming it is a motor which rotates at 742 rpm and in this project, the design and simulation verifications are done with this realization.

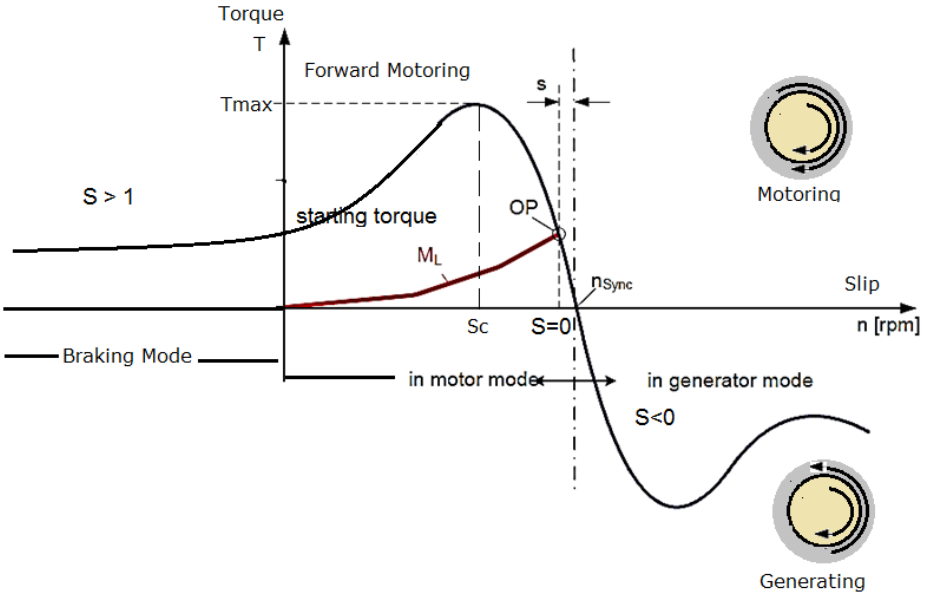


*Figure 1: Torque vs Speed Graph of Induction Machine*[1]

As stated earlier the rated torque can be calculated by dividing the output torque by the shaft speed as explained in (1) & (2).

[1] http://www.automationbasic.com/2018/01/torque-speed-characteristics-of.html

$$\omega_{shaft} = n_{shaft} * \frac{\pi}{30} = 77.7\ rad/sec \qquad (1)$$

$$T_{out} = \frac{P_{out}}{\omega_{shaft}} = 3217\ Nm \qquad (2)$$

For an induction machine, the magnetic loading (Bpeak) should be in range of 0.7T – 0.9T and the electrical loading in 30kA/m – 65kA/m. Thus, in this design, the magnetic loading is selected as 0.7T & electrical loading is selected as 55kA/m. With these loading rated, the tangential stress is calculated using eqn. (3) where the power factor is taken as 0.85. Then, the volume of the rotor is calculated as in (4) which enables us to reach $D^2L'$, (5).

$$\sigma_{tan} = \frac{A_{rms} * \hat{B} * PF}{\sqrt{2}} \qquad (3)$$

$$T_{out} = 2 * \sigma_{tan} * V_r \qquad (4)$$

$$D^2L' = 4 * \frac{V_r}{\pi} \qquad (5)$$

The aspect ratio, which is the ratio of axial length to the bore diameter, is taken as 0.35, so the shape of the motor is like a pancake. The aim was to increase the magnetic loading. It happens because reducing aspect ratio means reducing $DL'$ as a result of constant $D^2L'$. Therefore, we obtain smaller pole area, (6), so the magnetic loading increases, for the same flux per pole which is also stays constant due to the same induced voltage. Consequently, the bore diameter is obtained as 632 mm and effective axial length as 221 mm. Moreover, the air-gap is calculated using the eqn. (7). Knowing the air-gap the real axial length can be calculated as in eqn. (8).

$$A_{pole} = \frac{\pi * D * L'}{2p} \qquad (6)$$

$$\delta = 0.18 + 0.006 * P^{0.4} = 1\ mm \qquad (7)$$

$$L = L' - 2 * \delta = 219\ mm \qquad (8)$$

## Winding Design

For the winding design, the stator winding is designed for single layer. For different slots per pole per phase, q, values the slot number and slot pitch is calculated accordingly as shown in Table 2.

| q | Qs | Slot Pitch (mm) |
|---|---|---|
| 1 | 24 | 82.7 |
| 2 | 48 | 41.4 |
| 3 | 72 | 27.6 |
| 4 | 96 | 20.7 |
| 5 | 120 | 16.5 |
| 6 | 144 | 13.8 |

*Table 2: Slot Numbers and Slot Pitches*

Considering the rule of thumb that the slot pitch is between 7 mm and 45 mm, the slot number cannot be 24. Also, for the large power applications the slot pitch is greater. Therefore, the slot number is selected as 48 for this design. The resulting winding diagram is given below.

| 1 | 2 | 3 | 4 | 5 | 6 | 7 | 8 | 9 | 10 | 11 | 12 |
|---|---|---|---|---|---|---|---|---|---|---|---|
| A1 | A2 | -C1 | -C2 | B1 | B2 | -A1 | -A2 | C1 | C2 | -B1 | -B2 |

*Table 3: Winding Diagram Over a Pole Pair*

For this winding scheme, the MMF is plotted for three different case where the turn number is taken as one and the current peak value is also taken as one. Therefore, to calculate the actual MMF value, just the extension with NI coefficient is enough. The MMF plots of the cases are shown in Figure 2, 3 and 4. In both plots, the MMF is given for 12 slots which covers a pole pair. Thus, the plots just repeat itself for each pole pair.

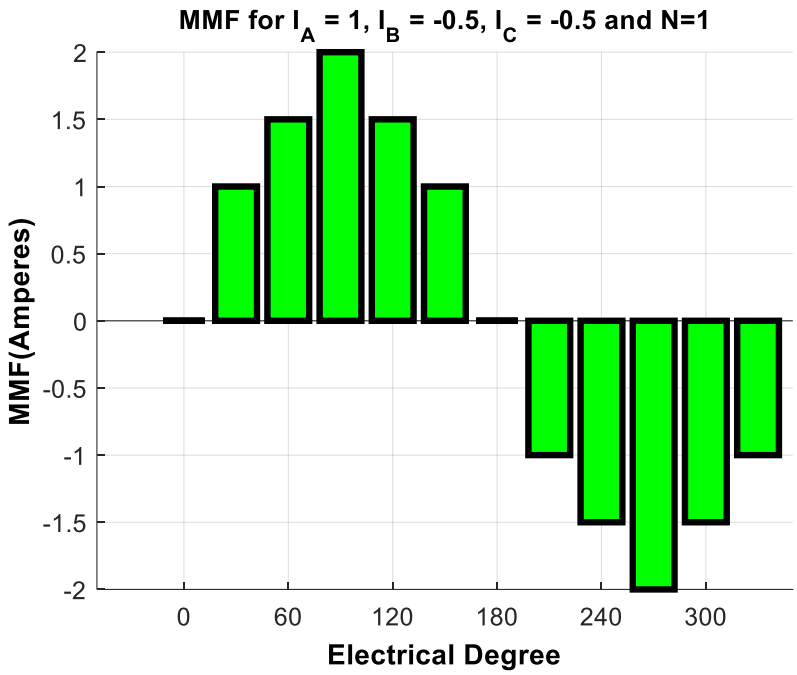


*Figure 2: MMF plot for Ia = 1 and Ib = Ic = -0.5*

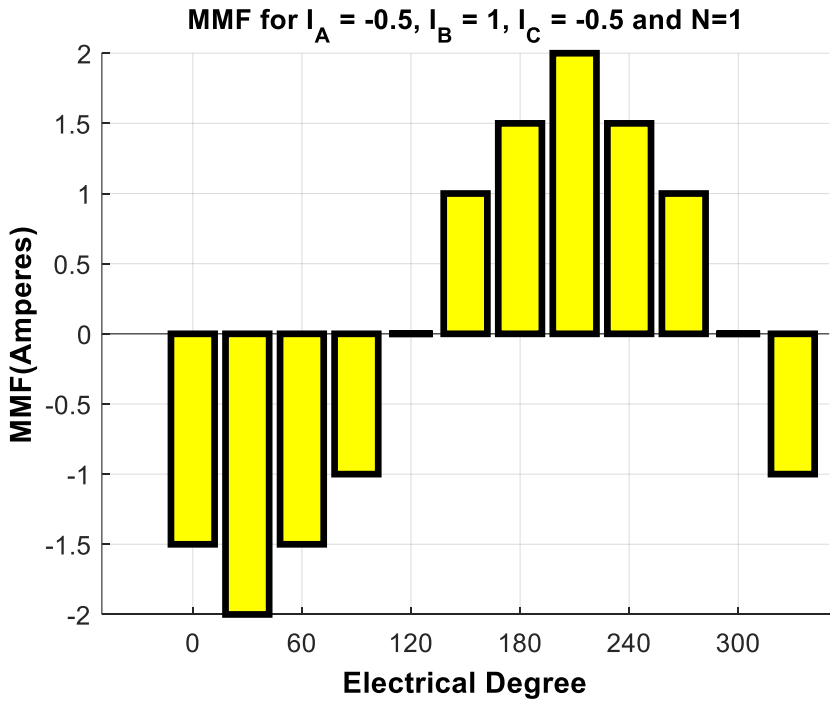


*Figure 3: MMF plot for Ib = 1 and Ia = Ic = -0.5*

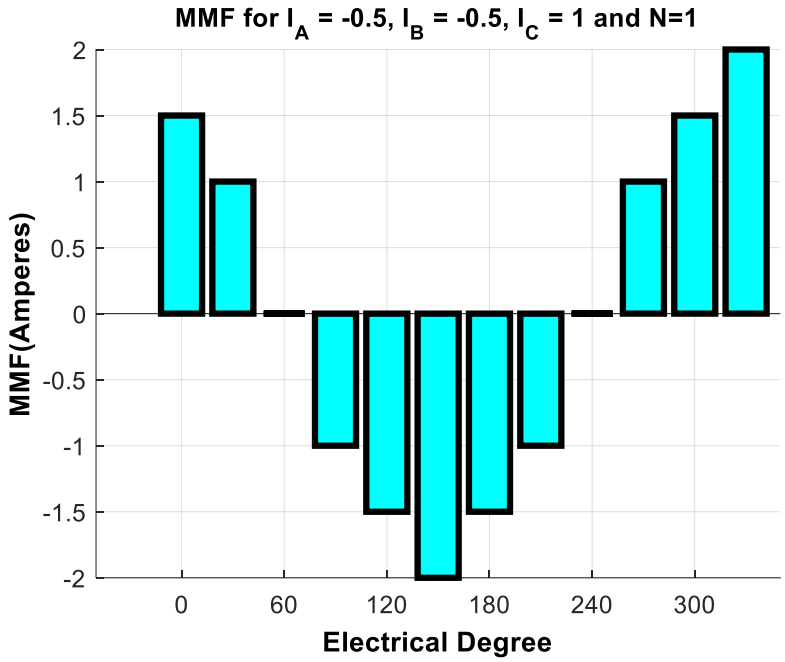


*Figure 4: MMF plot for Ic = 1 and Ib = Ic = -0.5*

Furthermore, the pitch factor, the distribution factor and the resulting winding factor are calculated as in eqns. (9), (10), (11) and given in Table 4. The coil span is 180 degrees whereas the slot angle is 30 degrees.

$$k_p(n) = \sin\left(n\frac{\lambda}{2}\right) \qquad (9)$$

$$k_d(n) = \frac{\sin\left(\frac{qn\alpha}{2}\right)}{qsin\left(\frac{n\alpha}{2}\right)} \qquad (10)$$

$$k_w(n) = k_p(n) * k_d(n) \qquad (11)$$

| Harmonic Order | Pitch Factor | Distribution Factor | Winding Factor |
|---|---|---|---|
| 1 | 1 | 0.9659 | 0.9659 |
| 3 | -1 | 0.7071 | -0.7071 |
| 5 | 1 | 0.2588 | 0.2588 |
| 7 | -1 | -0.2588 | 0.2588 |
| 9 | 1 | -0.7071 | -0.7071 |
| 11 | -1 | -0.9659 | 0.9659 |

*Table 4: Winding Factors*

Here, even though the winding factors for the harmonics are observed in very high amount in the line-to-line voltages they will not be that much high. As shown in eqn. (12), the magnetic harmonics in the air gap have different magnitudes. Since, the higher order harmonics have lower magnitudes, they will not be seen in induced EMF. That expectation is verified with 2D FEA results as given in Figure 5 and Figure 6.

$$EMF(n) = \frac{B(n)}{B(1)} * \frac{k_w(n)}{k_w(1)} * EMF(1) \qquad (12)$$

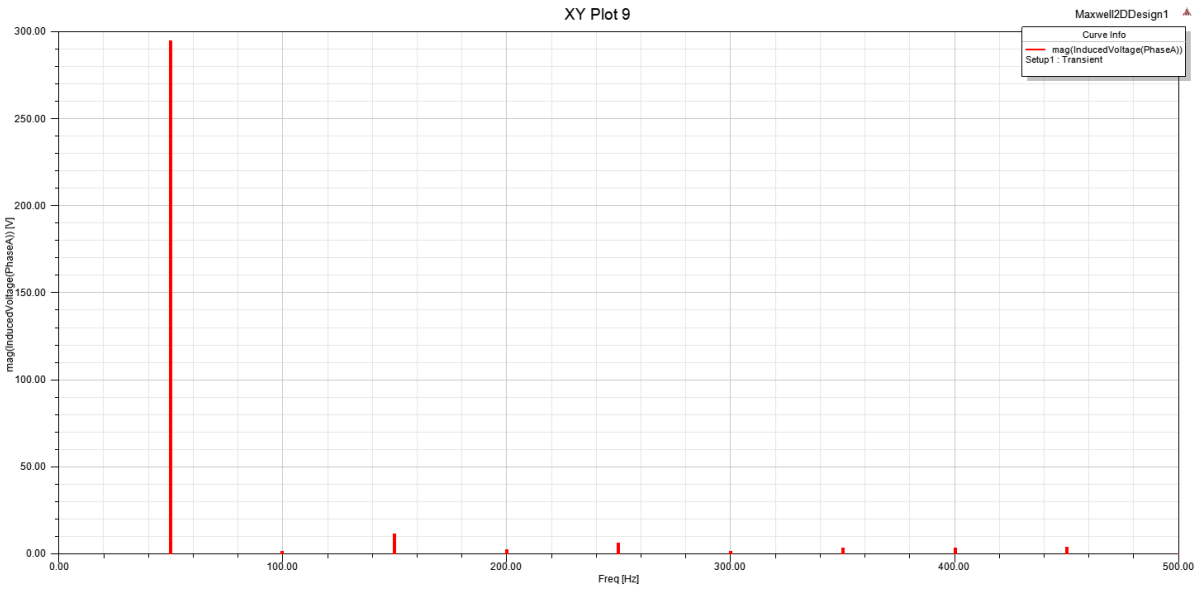


*Figure 5: FFT Result for Phase Induced Voltage*

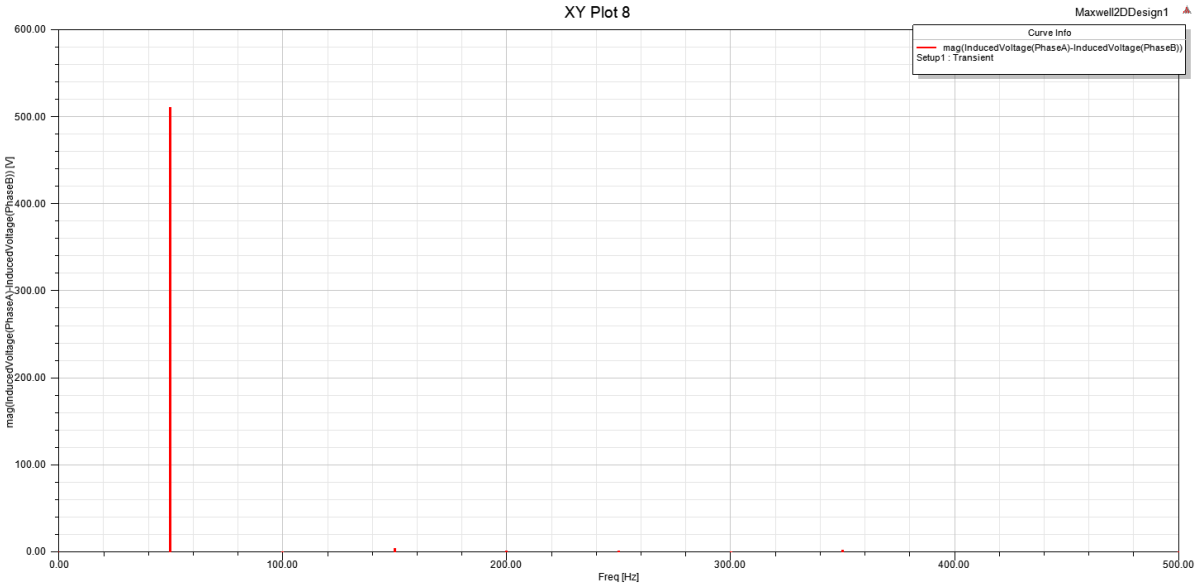


*Figure 6: FFT Result for Line to Line Induced Voltage*

Now, since the slot number is decided, it is possible to calculate series turn number in a slot. For this purpose, the flux per pole is calculated using the eqn. (13). Then, the series turn number in a phase is calculated with eqn. (14) and finally, the series conductor number per a slot is calculated in eqn. (15).

$$\emptyset_{pp} = \frac{B_{avg}}{A_{pole}} \tag{13}$$

$$N_{phase} = \frac{E_{rms} * 0.8}{4.44 * f * k_{w_1} * B_{avg} * A_{pole}} \tag{14}$$

$$N_{slot} = \frac{N_{phase}}{q * p} = 5 \tag{15}$$

For the wire selection, the current density is taken as 7 A/mm$^2$ considering the turbine will be cooled with a fan. Also, the efficiency is taken as 0.95 to find the apparent power so that the input current can be calculated. As given in eqn. (16) & (17), the input current is 446 Arms.

$$S_{in} = \frac{P_{out}}{PF * Efficiency} \qquad (16)$$

$$I_{stator} = \frac{S_{in}}{\sqrt{3} * V_{LL}} \qquad (17)$$

For the found input current, the required wire area is calculated as 63.8 mm$^2$. Since the cable area is thick too much, considering the skin effect, parallel conductors should be used. AWG 9 wire is selected with 6.63 mm$^2$ area, so 10 parallel conductors are used. Also it is assumed that each wires have insulations with 0.5 mm thickness. The resulting wire area is calculated again and with the fill factor, 0.6, the required slot area is calculated as in eqn. (18).

$$A_{slot} = N_{slot} * \frac{A_{wire}}{Fill\ Factor} \qquad (18)$$

## Lamination Dimensions

For the lamination material JFE_Steel_35HNE300 is selected from the Maxwell library. It is seen on the B-H curve of the material as shown in Fig. 7, the material can operate up to 1.8T without saturation and 1.5T can be considered as the safe limit.

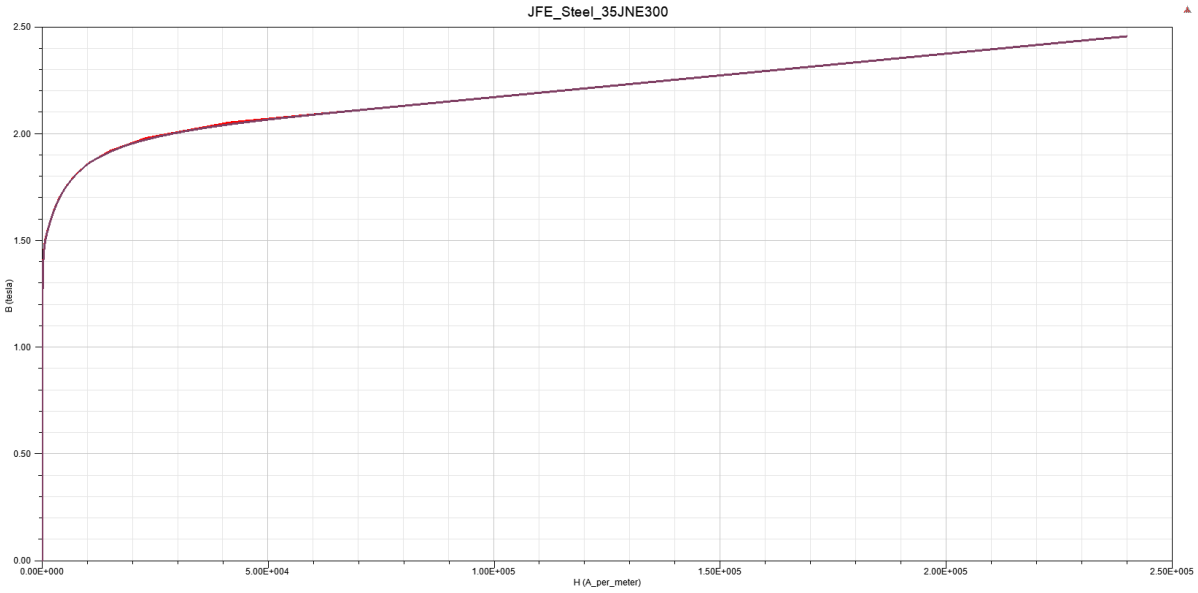


*Figure 7: B-H curve of the core*

The slot dimensioning is important to ensure the motor tooth is not saturated. If the tooth width is taken as small, it means that there will be saturation in the teeth which will affect the efficiency and heating. Tooth width is calculated using eqn. (19). In this equation, since we don't have any duck, $n_v$ is zero. Peak value of the tooth flux density is determined as 1.5T and stacking factor, $k_{FE}$, is considered as 0.96. Since the slot is designed with parallel side lines, the Bs2 and Bs1 is equal to slot pitch minus tooth width, Fig. 8. Here, $b_d$ is 20.3 mm and Bs1 is 21.1 mm where the slot pitch is 41.4 mm.

$$b_d = \frac{L' * \tau_u * \hat{B}_{airgap}}{k_{FE} * (L - n_v * b_v) * \hat{B}_d} \qquad (19)$$

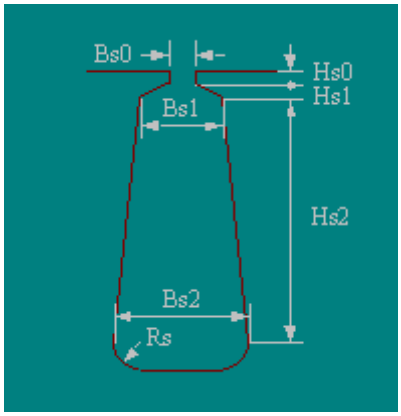


*Figure 8: Example Stator Slot*

Now, the slot area is calculated and slot width is calculated as well; thus, the slot depth can be calculated by dividing slot area by slot width and Hs2 is 48 mm. The remaining parts of the slot is determined using simulation results and they are as Bs0 is 15 mm, Hs0 is 3 mm and Rs is 0.

Another important dimension in the lamination is the thickness of the yoke. Since the flux flows in yoke over a pole it is thickness is very important for eliminating core losses and also thermal problems. The thickness of the yoke is calculated with eqn. (20) as 39 mm. The peak value of the flux density in the yoke is again considered as 1.5 T.

$$h_{ys} = \frac{\emptyset_m}{2 * k_{FE} * L * \hat{B}_{ys}} \qquad (20)$$

Rotor slot dimensions are determined more roughly than the stator slots. For this purpose, the laminations used in the project 2 are modified and the simulation results are taken into account. Here the Hs2 is 60 mm, Bs1 is 12 mm and Bs2 is 8 mm, Bs0 is 1.1 mm. These slots are filled with aluminium. Rotor slot number is selected as 61 which is advantageous for cogging torque and noise problems.

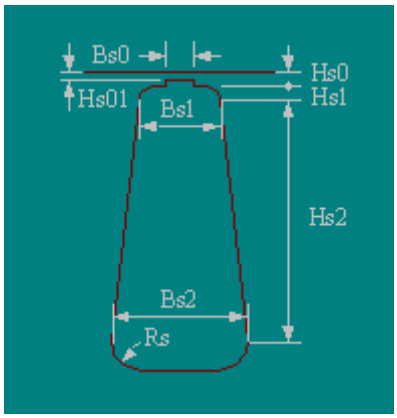


*Figure 9: Example Rotor Slot*

The core material has a density of 7700 kg/m$^3$ and the mass of stator core is calculated as 329 kg and mass of rotor core is calculated as 443 kg considering rotor has a shaft hole with 25 cm diameter. Copper mass is calculated ad 71 kg with considering mean path as given in eqn. (21). With this mean path the copper resistance also calculated as 102 m-ohm. Due to the 10 parallel strands, the resistance is low relatively.

$$l_{mean} = 2 * L + \tau_p * 2 * \pi \qquad (21)$$

## C. SIMULATION ANALYSIS

Firstly, the design is verified in the RMXPRT platform. The results are given in the Table 5. The green elements are considered as matched very correctly while the orange ones are considered it would be better if they were closer. However, in general, the analytical results are matched with simulation results successfully. There is a deviation in the yoke flux density results. The RMxprt result says the flux density in the stator yoke is greater than the expected one. However, since the yoke is not saturated the yoke thickness is remained as same. Similarly, even though the fill factor has a deviated result, since the simulation result is better than expected, the slot dimensions are not changed.

| | Analytical Result | RMxprt Result |
|---|---|---|
| Electric Loading (kArms) | 55 | 52.5 |
| Magnetic Loading (T) | 0.7 | 0.699 |
| Power Factor | 0.85 | 0.855 |
| Efficiency | 0.95 | 0.94 |
| Output Power (kW) | 250 | 244 |
| Shaft Torque (Nm) | 3217.4 | 3150 |
| Shaft Speed (rpm) | 742 | 742 |
| Stator Current (Arms) | 446 | 434 |
| Stator Phase Resistance (ohm) | 0.01 | 0.012 |
| Copper Loss (kW) | 6.11 | 6.65 |
| Core Loss (kW) | 1.77 | 2.4 |
| Tooth Flux Density (T) | 1.5 | 1.48 |
| Yoke Flux Density (T) | 1.5 | 1.65 |
| Fill Factor | 0.6 | 0.5 |
| Stator Current Density ($A/mm^2$) | 7 | 6.55 |
| Stator-Rotor Mass (kg) | 224-363 | 329-443 |
| Copper Mass (kg) | 75.8 | 71 |

*Table 5: Comparison Table of Analytical Results with RMxprt Results*

In Figure 10, the torque vs speed graph is plotted for motoring region. In Figure 11, power factor vs output power is given. This is a nice plot to see and estimate where the induction generator should be operated considering the grid reactive power limitations.

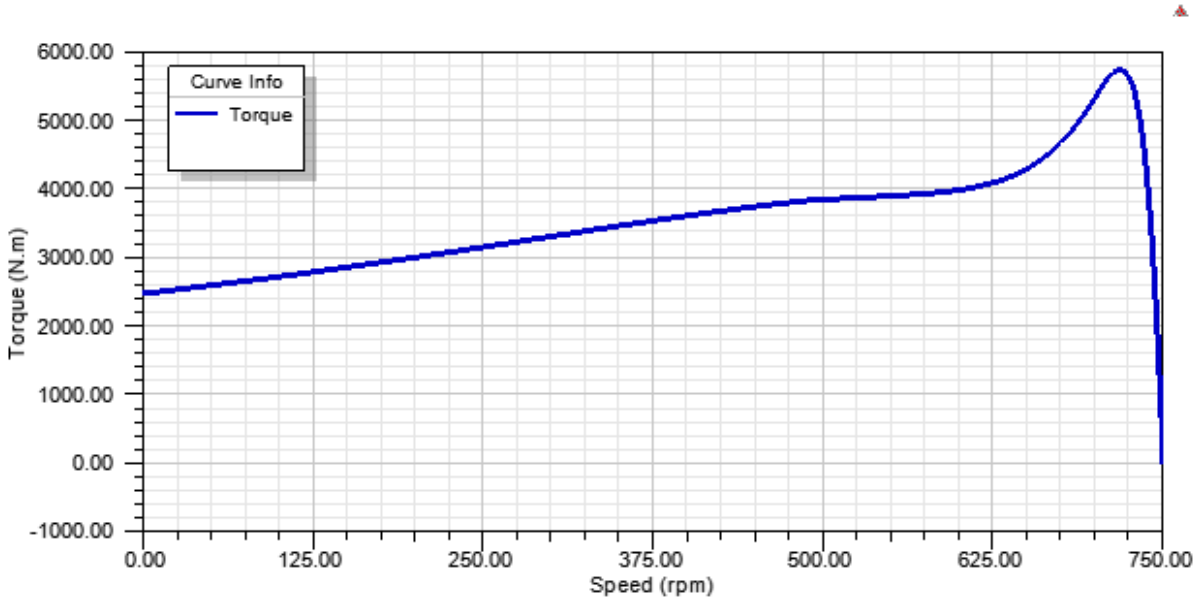


*Figure 10: Torque vs Speed Graph*

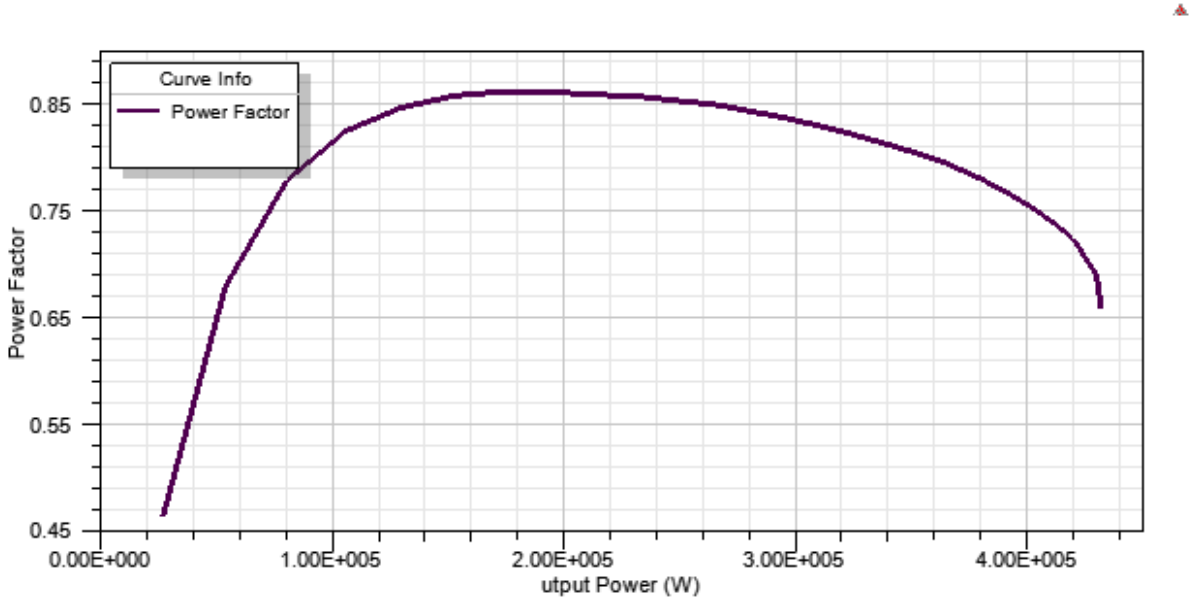


*Figure 11: Power Factor vs Output Power*

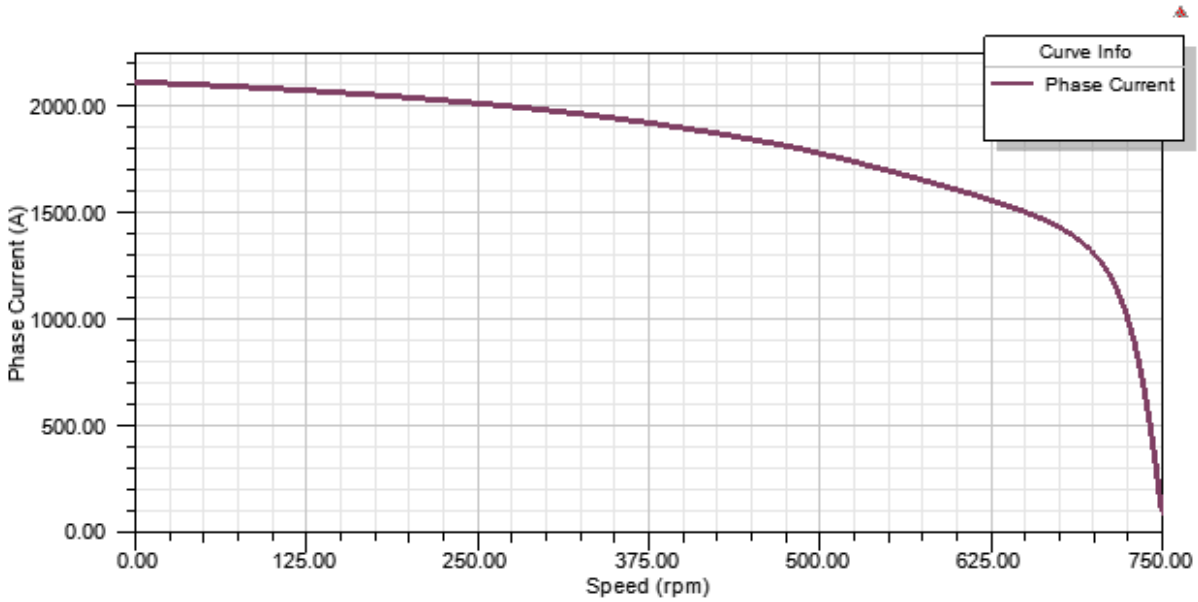


*Figure 12: Phase Current vs Speed Graph*

Another important plot is phase current vs speed graph which is shown in Fig. 12. For starting moment an induction motor always sinks much more current than the rated value. So, if this machine is supplied with a power electronics circuitry, then the circuitry must be designed considering the inrush current as well.

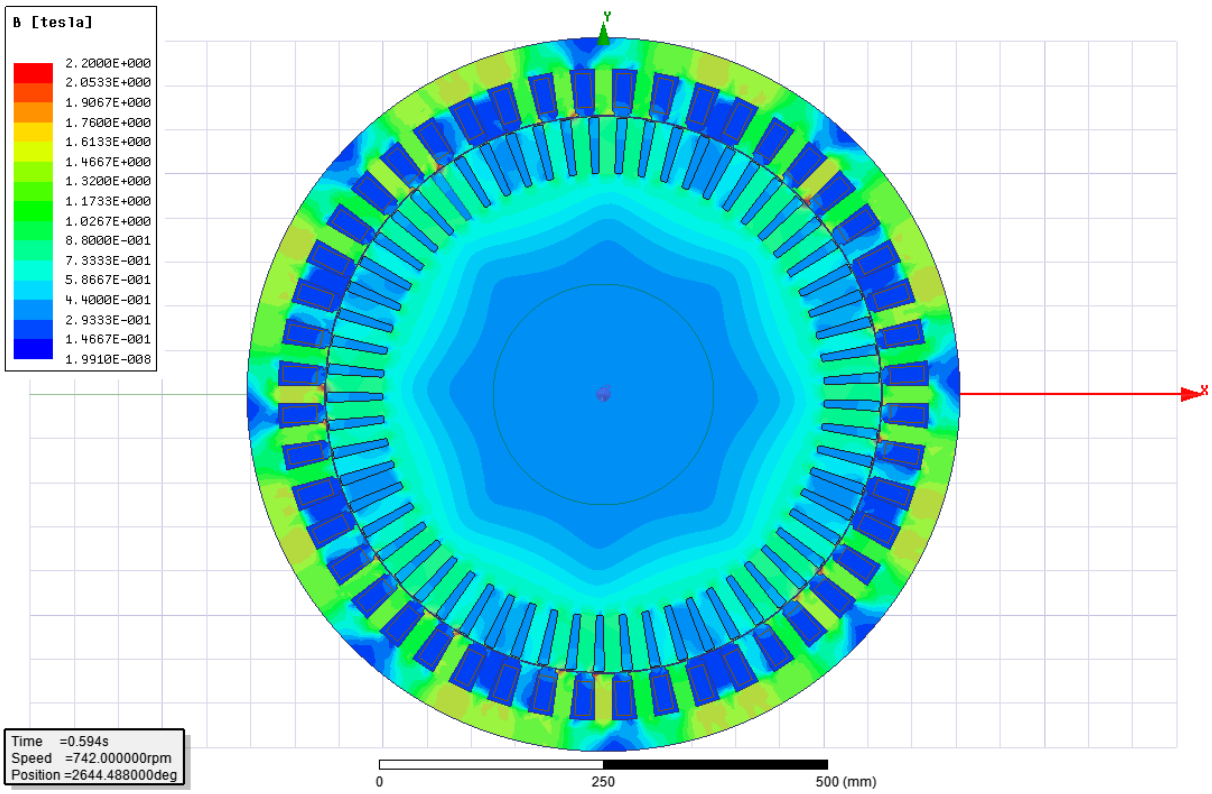


*Figure 13: Flux Density of Machine*

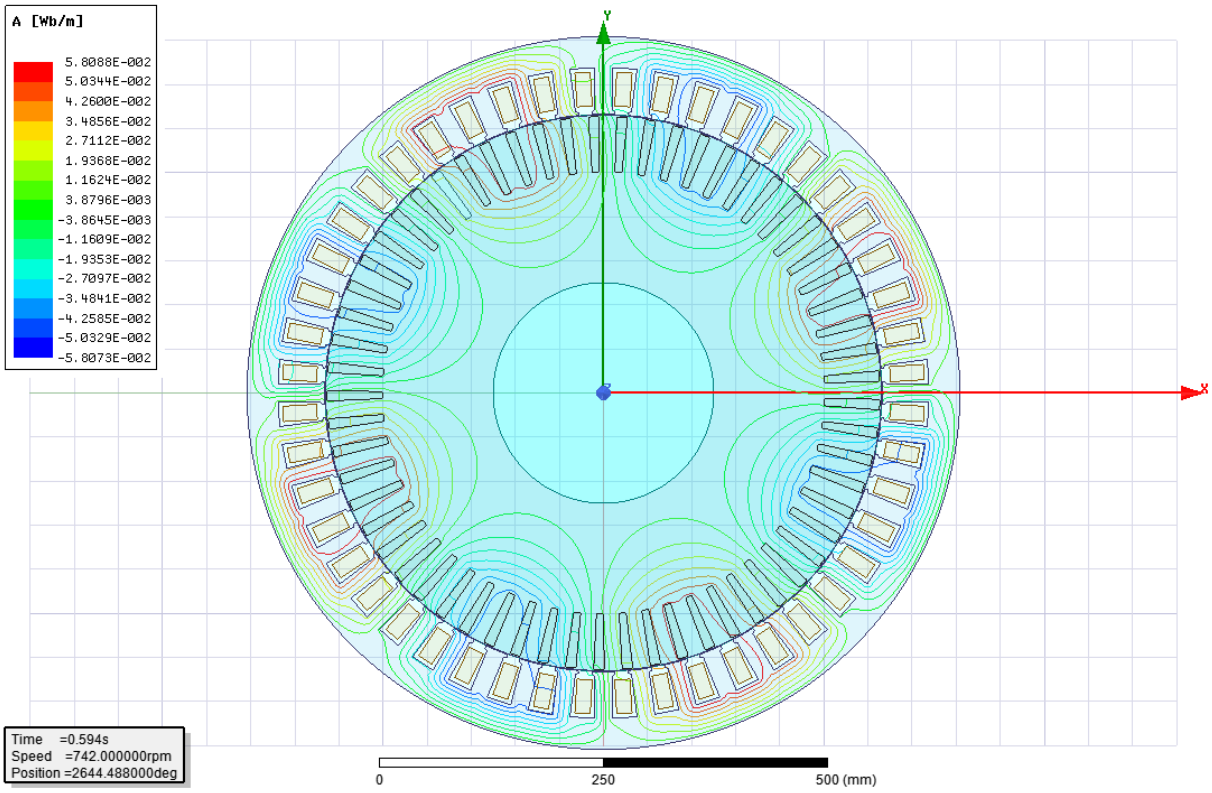


*Figure 14: Flux Lines of The Machine*

In Figure 13 and 14, the flux density and flux lines are plotted over the whole machine respectively. In Figure 13, it is seen that the machine is operating without saturation in teeth or yokes. The limitation was 1.8 T for the core material and the operation is performed in the safe region. In Figure 14, the flux lines are visible. Since this is an 8 pole machine, we observe the fluxes are not flowing through the yoke completely. It is important because if this would be a 2 pole machine, we will observe the fluxes flowing through the half of the yoke which forces designer to make yoke thick larger in order to ensure unsaturated operation.

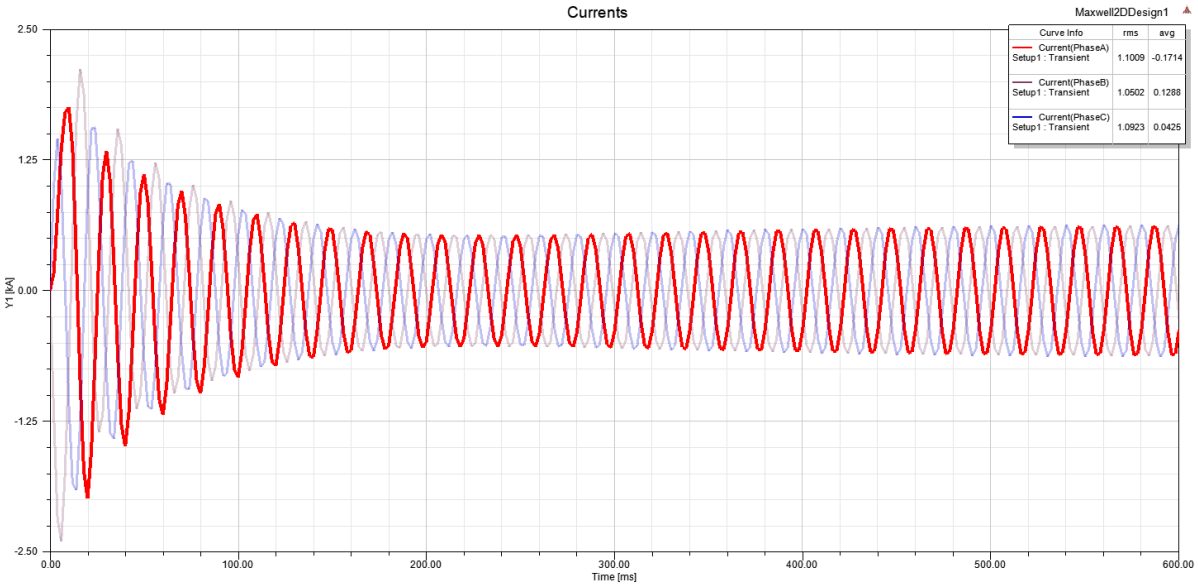


*Figure 15: Phase Currents*

In Figure 15, the phase currents are given in transient. Here, clearly we see the inrush current which is sinked when the motor is just starts to accelerating.

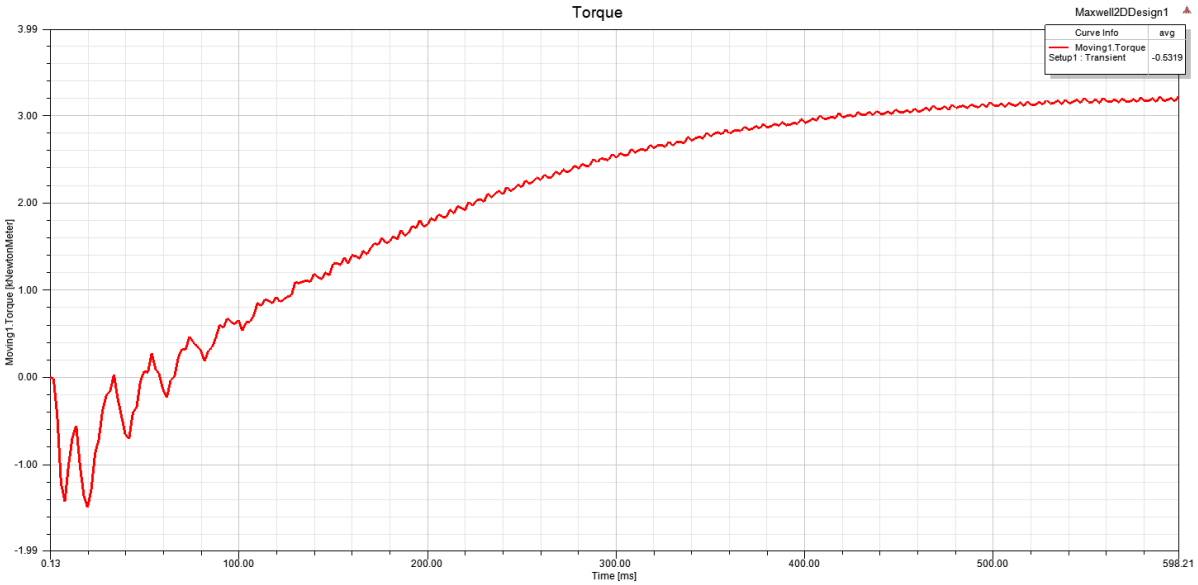


*Figure 16: Transient Torque Graph for Rotor Slot Number is 61*

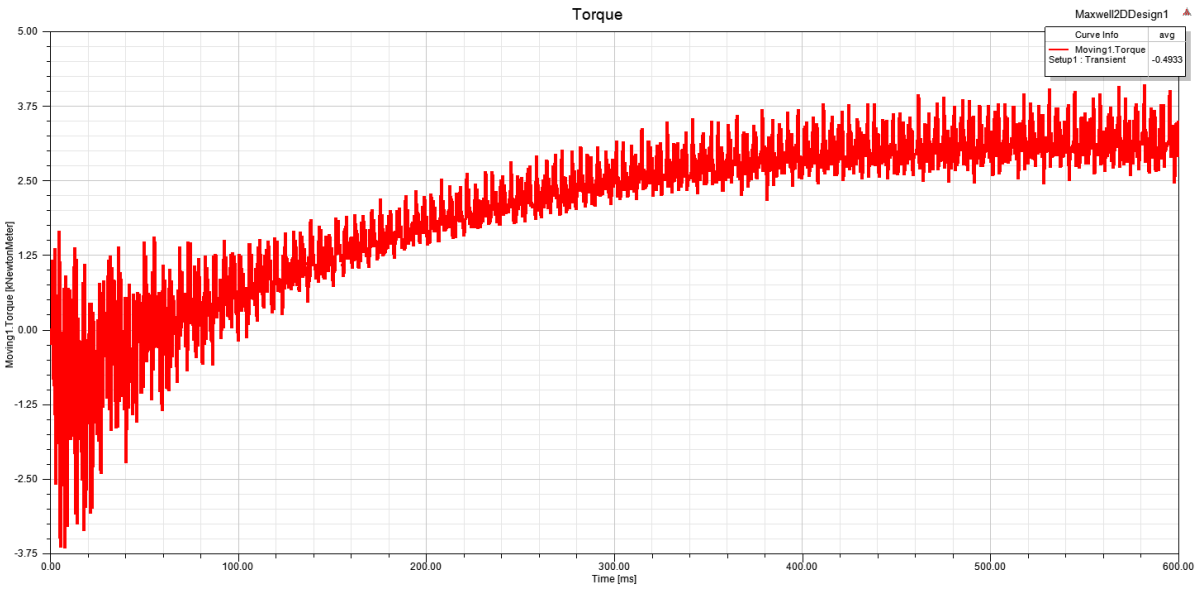


*Figure 17: Transient Torque Graph for Rotor Slot Number 64*

In Figure 16 & 17 shows very clearly how important the slot number selection on the cogging torque. Even though the rotor slots are skewed, if the slot numbers are selected as a wrong combination, we observe much more ripple on torque which is the cogging torque. In Figure 17, since the rotor slot number is equal to Qs + 2*p, the torque is too much distorted and it is harmful for motor mechanical elements in the long term and also it is absolutely not fine for the load. On the other hand, if the combination is selected as properly like in Fig. 16, the resulting torque will be clear and the motor will have longer safe operation time.

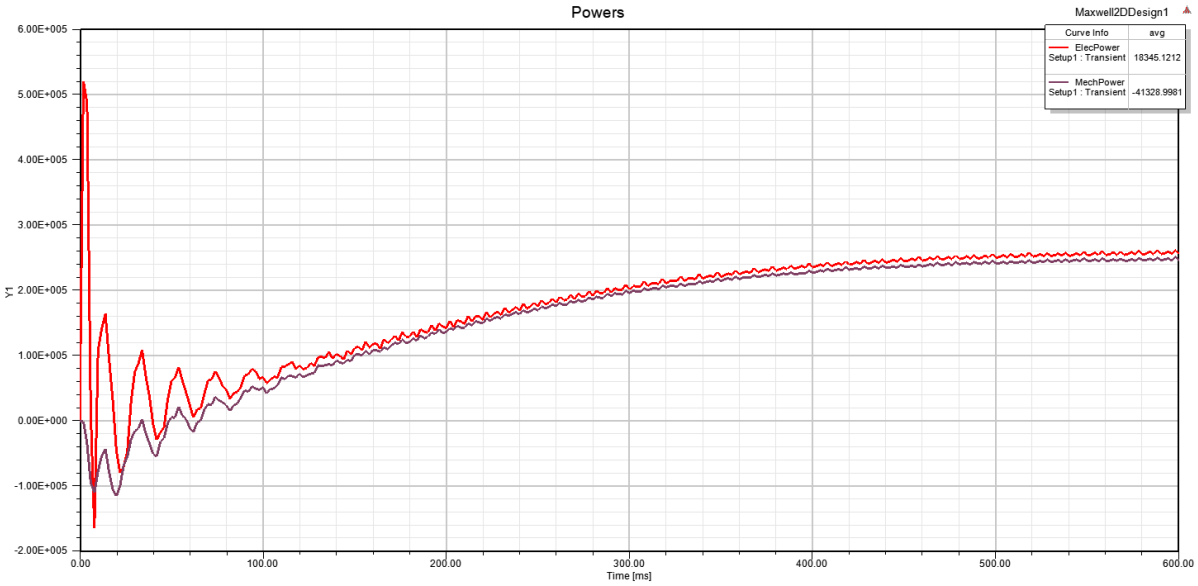


*Figure 18: Electrical Power and Mechanical Power Graph*

Since the simulations are performed as motoring, we observe larger electrical power than the mechanical power. The difference of these powers are lost in the motor electrically and mechanically. If the operation was simulated in generator mode, we would see the mechanical power is larger than the electrical power. Another important point is that when the motor is just started to acceleration, it sinks large amount of power whereas it cannot transfer the power to shaft. This is in comply with current graph as expected.

## D. CONCLUSION

In this project, a wind turbine generator design is performed. As a first step, the induction generator parameters and dimensions are calculated analytically. In analytical calculations, the main dimensions of the machine are calculated. Then, the winding design is completed and slot dimensions are determined considering the saturation limits. Secondly, the design is verified in RMXPRT platform and torque-speed, phase current-speed graphs are obtained in this platform. Afterwards, in 2D design transient analysis is completed and the torque, phase currents are obtained with respect to the time. Lastly, the flux densities are observed verifying the core is not saturated. Also, the cogging torque is compared for different rotor slot number and it is shown that the rotor slot number has to be selected by considering the disadvantageous combinations to reduce the cogging torque and noise problems.